



## Original Paper

# High molecular weight guar gum assisted settling of fine solids in diluted bitumen: Effect of solvents

Camila Santander, Jing Liu, Xiao-Li Tan, Qi Liu, Hong-Bo Zeng\*

Department of Chemical and Materials Engineering, University of Alberta, Edmonton, AB T6G 1H9, Canada



## ARTICLE INFO

## Article history:

Received 23 December 2020

Accepted 13 April 2021

Available online 10 September 2021

Edited by Xiu-Qiu Peng

## Keywords:

Non-aqueous extraction

Fine solids

Guar gum

Agglomeration

Settling

## ABSTRACT

As water-based extraction technologies for producing bitumen from oil sands have received increasing environmental concerns, developing non-aqueous extraction (NAE) technique is of both fundamental and practical importance. However, the relatively high concentration of fine solids trapped in the extracted bitumen presents an obstacle for pipeline transport as well as upgrading and refining downstream. This research attempts to provide a solution to fine solids removal without using synthetic additives or affecting bitumen recovery from NAE process. Herein, naturally hydrophilic additives (i.e., water and high molecular weight guar gum (HGG) produced from *Cyamopsis tetragonoloba* L. Taup.) were introduced to promote the settling of fine solids suspended in bitumen-solvent solution, and the effects of solvents (i.e., toluene, cyclohexane and their mixtures) were systematically investigated. Aggregate size distribution analyzed by the focused beam reflectance measurements confirmed that the addition of water and HGG could promote the agglomeration and settling of fine solids in all solvents studied. However, the size range and quantity of the agglomerates vary significantly with the solvent's aromatic character. Solvent mixtures demonstrate a superior performance on removing fine solids from bitumen over single solvent. Specifically, in a 3:2 toluene/cyclohexane mixture, the solid content was lowered from 0.66 wt% to 0.09 wt%.

© 2021 The Authors. Publishing services by Elsevier B.V. on behalf of KeAi Communications Co. Ltd. This is an open access article under the CC BY license (<http://creativecommons.org/licenses/by/4.0/>).

## 1. Introduction

Non-aqueous extraction (NAE) of bitumen from oil sands is a promising alternative method to hot water extraction (HWE), in which organic solvents are used instead of water to recover bitumen from oil sands ores. Light hydrocarbon solvents such as cyclohexane, heptane, toluene and their mixtures have been investigated intensively as suitable solvents in the NAE process (Hall et al., 1983; Nikakhtari et al., 2013; Sparks et al., 1988). In general, aromatic or cyclic solvents can yield a high bitumen recovery because of their strong solvation power to the bitumen components (Nikakhtari et al., 2013). However, the bitumen produced from NAE process presents a significant challenge to downstream operations due to the migration of a high number of fine solids from oil sands ores to bitumen products (Hall et al., 1983; Liu et al., 2008; Nikakhtari et al., 2014; Sparks and Meadus, 1981). Those fine solids are mainly clay fractions (<2 μm). Even though most clay minerals are naturally hydrophilic, their surface

wettability could be altered to become less hydrophilic or more hydrophobic by the adsorption of the organic components due to their burial or immersion in an organic matter environment (e.g., asphaltenes, resins or humic materials) (Smith et al., 2011; Zahabi et al., 2012). Such modification affects their separation from the organic liquid medium. The aforementioned characteristics of clay minerals in bitumen limit conventional centrifugation or filtration from being effective in large scale applications.

The addition of a small amount of water to the NAE bitumen-solvent system triggers aggregation of fine solids (Anderson, 1985; Liu et al. 2019a, 2019b; Yan et al., 2001), which are clays that have adsorbed asphaltenes in their surface (Liu et al., 2017). Thus, modifying the surface of the fine solids to reduce its hydrophobicity has been a topic of research aimed to lower the fine solids content in NAE bitumen (Liu et al., 2003; Lu et al., 2016; Tan et al., 2009; Tan et al., 2013). However, this process is complicated by the inhomogeneity of the organic components coating, and the varying contents of swelling versus non-swelling clays depending on the source of oil sands (Geramian et al., 2016; Hooshier et al., 2012; Hooshier et al. 2012, 2012). The addition of ionic liquids can effectively remove the bitumen coating of the fine solids, therefore

\* Corresponding author.

E-mail address: [Hongbo.Zeng@ualberta.ca](mailto:Hongbo.Zeng@ualberta.ca) (H.-B. Zeng).

changing the hydrophobicity, due to strong electrostatic interactions between the clays and the ionic liquid. However, high toxicity and poor recovery of the ionic liquid restrict the application of this method (Hogshead et al., 2011; Painter et al., 2010).

Modifying the aromatic character of the organic solvent by increasing the concentration of alkanes or cyclo-alkanes (e.g., heptane and pentane) could result in the settling of fine solids and asphaltene, similar to paraffinic bitumen froth treatment. However, a trade-off is undesirable loss of bitumen recovery (Liu et al., 2019; Natarajan et al., 2011; Pal et al., 2015). Therefore, a mixture of toluene, a widely used aromatic solvent with a rigid structure, and cyclohexane, a highly hydrophobic saturated hydrocarbon ring, commonly used in NAE (Pal et al., 2015; Tian et al., 2019), is used in this work in addition to hydrophilic additives such as guar gum.

Guar gum is a natural polysaccharide, extracted from *Cyamopsis tetragonoloba* L. Taup. It has long been established in the food industry as a thickener or a binder and in wastewater treatment as a flocculant (Gupta and Ako, 2005; Sharma et al., 2018; Thombare et al., 2016). It is a polymerized chain based on galactomannan monomers with a high molecular weight (approximately 500K g/mol) and strong hydrophilic character because of the presence of many hydroxyl groups (Pal et al., 2007). For the sake of simplicity, the high molecular weight guar gum is expressed as HGG, and the structure of HGG is shown in Fig. 1. HGG shows high solubility in water and water-miscible solvents such as glycols and alcohol (Mahmoud, 2000). It has been reported that HGG presents good affinity with glucose, maltose and other oligosides because of multiple hydrogen bonding interactions (Narchi et al., 2009).

In theory, HGG could be effective to aggregate bituminous fine solids due to its high molecular weight and the hydrogen bonds formed between its hydroxyl groups and connate water layer of the fine solids or mineral surface (Liu et al., 2017; Ma and Pawlik, 2007; Tan et al., 2013). However, in organic solvents, HGG particles settle quickly, resulting in a decreased probability of aggregate formation with fine solids (Hasan and Abdel-Raouf, 2018). Moreover, the hydrophilic HGG particles might interact with each other solely through active hydrogen bonds to form homo-aggregation instead of hetero-aggregation with fine solids (Pal et al., 2015). The growth of aggregates as well as collision frequency depend on the size of the colliding particles, particle concentration and surface charge in addition to the hydrodynamic conditions (Chakraborti et al., 2003; Li et al., 2016; Liu et al., 2003). By using focused beam reflectance

measurement (FBRM), the kinetics of aggregate formation and size evolution of particles can be tracked (Park et al., 2014; Schäfer et al., 2002; Tadayyon and Rohani, 1998; Vajihinejad and Soares, 2018). Therefore, this research work attempts to develop an efficient, environmentally friendly and cost-effective approach to separate fine solids from the NAE bitumen by using HGG in a solvent mixture of toluene and cyclohexane.

## 2. Materials and methods

### 2.1. Materials and equipment

Athabasca bitumen that had been processed to remove sand and water and contained 0.66 wt% of fine solids was provided by an oil sands operator in Western Canada. HPLC grade toluene and cyclohexane (certified ACS grade, > 99%) from Fisher Scientific were used as the organic solvents in this study. HGG (Mn ~ 500K, Everland Natural products) was used for aggregate formation. Milli-Q water (Millipore deionized with a resistance of  $\geq 18.2$  M $\Omega$  cm) was applied as the water additive in the sedimentation tests as well as being used to dissolve the HGG. For solid content determination by hot filtration nylon Whatman membrane filters (pore size 0.45  $\mu$ m and diam. 47 mm) were used.

Focused beam reflectance measurement (FBRM G400, Mettler Toledo, USA) was used to track the aggregation of particles in real-time. The probe uses laser light backscatter technology to supply, in real time, chord length distribution (CLD) as the laser light randomly traverses particles passing through the measurement zone. As the beam crosses the surface of a particle or particle structure, light from the beam is backscattered into the probe. The duration of each reflection is multiplied by the velocity of the scanning beam, resulting in a chord length (Autochem, 2006; Park et al., 2014). Chord length counts were grouped (No weight: number density) into size intervals to yield a graphical distribution (Tadayyon and Rohani, 1998). The measurement range is 0.5–2000  $\mu$ m (Autochem, 2006).

### 2.2. HGG settling curve

DI water diluted HGG (200 mg/L) was added to DI water, toluene or cyclohexane in a concentration of 0.5 wt%, respectively. Each solvent-diluted sample underwent sonication for 5 min followed by 10 min of agitation with a magnetic stirrer (1100 rpm), before being transferred to a 100 mL graduated cylinder. During the sedimentation process, the changes of mudline location in the cylinder (mL) were recorded as a function of settling time (s), and the slope of the linear part of the settling curve was used to determine the initial settling rate (ISR).

### 2.3. Water droplet size in pure toluene and cyclohexane

For the size measurement of water droplets in pure toluene and cyclohexane, the FBRM measurement was performed by immersing the probe into a 250 mL beaker of pure solvent and 0–3 vol% of water were added at constant stirring speed of 1100 rpm. The corresponding chord length of the water droplet in the solvent is recorded and presented graphically as a size distribution figure.

### 2.4. Water droplet effect on bitumen fine solids aggregation

A solution containing 1 part bitumen and 25 parts solvent (by volume) was prepared in a 250 mL beaker, sonicated for 5 min and agitated using a magnetic stirrer (1100 rpm) for an additional 10 min. Then, water was introduced to the solution to a concentration of 0–3 vol% while maintaining the stirring speed. The FBRM

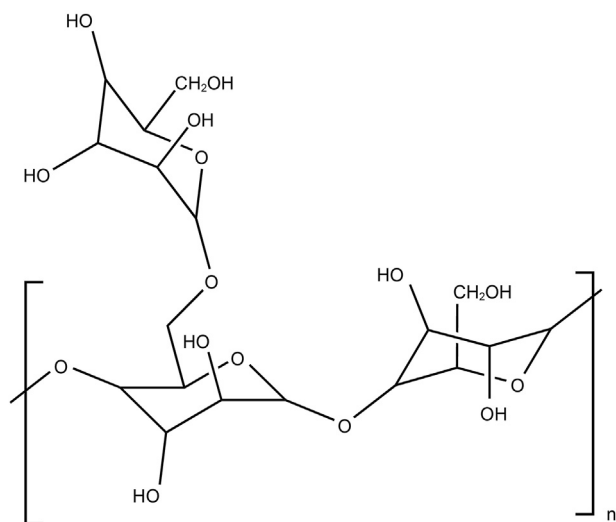


Fig. 1. Reported structure of high molecular weight guar gum (HGG) (Sharma et al., 2018).

probe was immersed to the solution to measure any detected particle size prior to the addition of water.

### 2.5. FBRM measurement of water and HGG induced aggregate formation

The effect of aromaticity on aggregate formation is studied by FBRM. Mixtures of toluene/cyclohexane (T/Ch), in 3:2 and 2:3 v/v ratios were prepared. The FBRM probe was immersed into the 250 mL beaker containing the desired solvents mixtures, and a stock aqueous solution of HGG at 200 mg/L was added slowly in a 1 h period to a concentration of 0.5–7.0 vol%. Any formed aggregates were monitored by the FBRM.

### 2.6. FBRM measurement of water and HGG induced aggregate formation before and after settling

Monitoring the settling of fine solid-HGG aggregates by FBRM at high stirring speed, in addition to the elevation of the probe in relation to bottom of the beaker presents challenges. Therefore, to track the formation of aggregates and their settling in a dynamic environment, the stirring speed was decreased from 1100 rpm to 20 rpm. Specifically, the slurry of bitumen/solvents with 0.75 vol% of DI water and HGG solution were stirred at 1100 rpm for 10 min followed by a change in the stirring speed to 20 rpm. Two measurements were taken: the first one was taken immediately after the stirring speed was reduced, and the second measurement was performed after 5 min mixing at 20 rpm.

### 2.7. Solid content determination by ashing and hot filtration

The fine solids content in the supernatant after 30 min of settling was determined by an ashing method as described below. If the ashing results indicated that the solid content was below 0.2 wt %, a hot filtration protocol was used to more accurately determine the fine solid content.

**Ashing method:** This method determines ash content in distillate and residual fuels, gas turbine fuels, crude oils and other petroleum products. The term “ash” includes undesirable impurities or contaminants that are incombustible, also known as mineral particles or fine solids. In brief, about 3 g accurately weighed sample was poured in previously weighed crucibles, said crucibles have been dried in a muffle furnace at 775 °C before weighing. The crucibles are put inside the muffle furnace for 12 h at 80 °C to ensure any residual solvent has been removed from the sample. The weight of the solvent-free bitumen crucibles is recorded followed by introducing them back into the muffle furnace and set to burn at 775 °C for 3 h. The crucibles are cooled and weighed ([International Petroleum Test methods, 2008](#)).

**Hot filtration:** This method determines the sediment in crude oils by membrane filtration. In a clean 250 mL beaker containing 100 mL of toluene, 1 g of a solvent free sample is placed. The beaker is placed on a hot plate with an external temperature probe controlling the temperature at 90 °C. A second hot plate with external temperature control probe was used to heat another beaker of 300 mL of toluene at the same temperature. When the desired temperature is reached and a dried and weighed filter is placed in the vacuum set-up, the filtration is started transferring the hot sample into a filtration flask. Hot toluene is transferred to the sample beaker and is used to rinse all the sample into the filtration flask. When the entire sample has been filtered, the vacuum is left on for an additional 10 min to dry out the filter paper. The filter paper with residue is dried at 115 °C and weighed to give the final result ([American Petroleum institute, 2015](#)).

## 3. Results and discussions

### 3.1. Water droplet size in pure toluene and cyclohexane

Certain amount of water was added to toluene or cyclohexane stepwise from 0.5, 1, 2 to 3 vol% at constant stirring speed of 1100 rpm while the FBRM probe was immersed in the solution to measure droplet size. The results are shown in [Fig. 2](#). As can be seen, droplet stability varies significantly between the two solvents. Overall, the size of water droplets in cyclohexane is predominantly in the range of 10–30  $\mu\text{m}$  with a unimodal distribution, and water cannot be dispersed well in cyclohexane (a phase separation might occur even at such high mixing speed). In toluene, a bimodal distribution was observed with increasing DI water concentration. The peak in the 10–30  $\mu\text{m}$  range is similar to cyclohexane, indicating unstable emulsion droplets, while peaks in the range of 1–10  $\mu\text{m}$  likely indicate the stable water-in-oil emulsion.

### 3.2. Water droplet size in bituminous toluene and cyclohexane

Each solvent is separately added to bitumen in a 1:25 bitumen to solvent volume ratio followed by the addition of water droplets. [Fig. 3](#) shows the FBRM measurement results in this system. Compared with [Fig. 2](#), a shift to lower chord length is observed. This may be caused by the presence of fine solids in the bitumen, and/or by the emulsion stabilization capability of the bitumen components. Without the addition of water (black line), the size distribution of fine solids is comparable in both solvents with a mean value of ~5  $\mu\text{m}$ . By adding water, the results start to differ accordingly. In the cyclohexane/water/bitumen system ([Fig. 3a](#)), aggregate size distribution shifted to large size gradually by increasing the water concentration. All fine particles are in a water-in-oil emulsion form at above 2 vol% water concentration, resulting in a disappearance of unimodal distribution of fine particles. In contrast, addition of water has two contributions to the toluene/bitumen ([Fig. 3b](#)): (1) A similar chord length peak to fine solids from 1 to 20  $\mu\text{m}$  with much higher counts. (2) Similar to water droplets in pure toluene, between 10 and 40  $\mu\text{m}$  but with a much high counts intensity. The overall results suggest that the water forms a relative stable emulsion in bitumen/toluene/fine solids as the size of water droplets are smaller than that in cyclohexane.

### 3.3. HGG settling curve

HGG sedimentation tests were conducted in DI water, toluene and cyclohexane by following a previously reported approach ([Liu et al., 2019](#); [Park et al., 2014](#)), and the results are shown in [Fig. 4](#). In toluene and cyclohexane, most of the HGG settled to the bottom of the graduated cylinder within 1 min of the test, and the settling reached equilibrium after 2 min, while HGG in water formed a stable suspension.

Studies related to HGG have reported its solubility in water and other solvents with high content of hydroxyl groups ([Tan et al., 2013](#); [Towle and Whistler, 2012](#)), but none of the studies have been performed in non-polar solvent. It is expected that the solubility of HGG in toluene and cyclohexane is extremely low, if not insoluble, thus the concentrations of HGG particles in solvents are essentially same. As shown in [Fig. 4](#) and [Fig. S1](#), the settling rate of HGG in toluene, cyclohexane and toluene/cyclohexane mixtures are similar indicating that aromaticity of solvent is not a factor to influence the settling of HGG particles in the solvents.

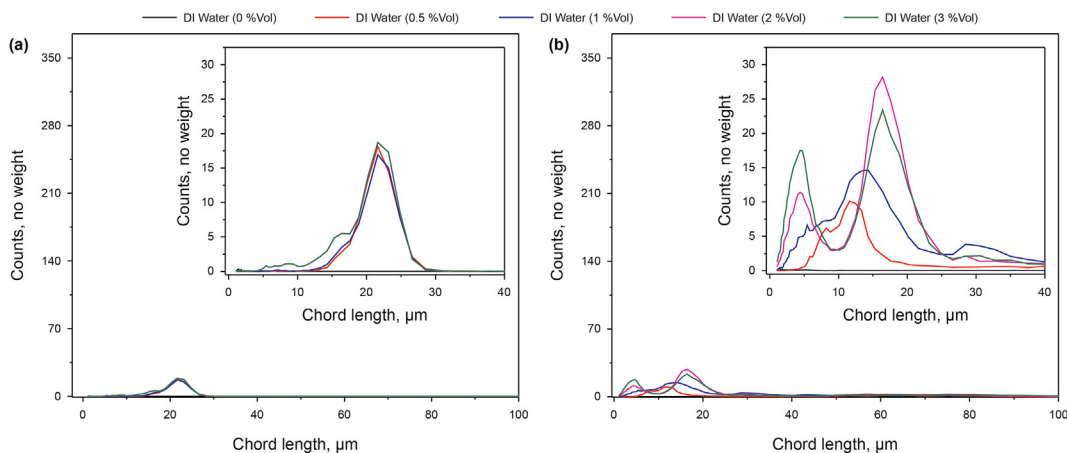


Fig. 2. FBRM measurements of DI water droplet formation in a) cyclohexane and b) toluene. Inserts: close-up look at Fig. 2a and b.

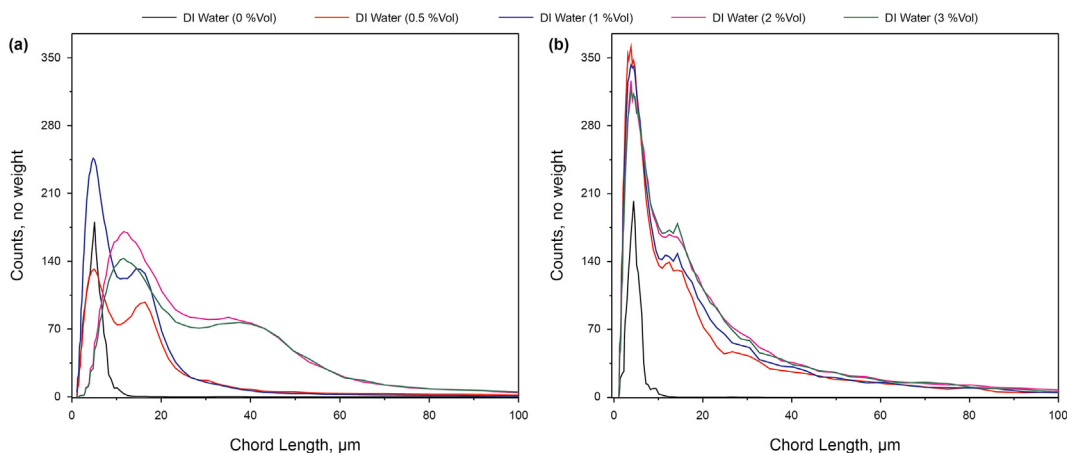


Fig. 3. FBRM measurements of DI water droplet size in bituminous a) cyclohexane and b) toluene.

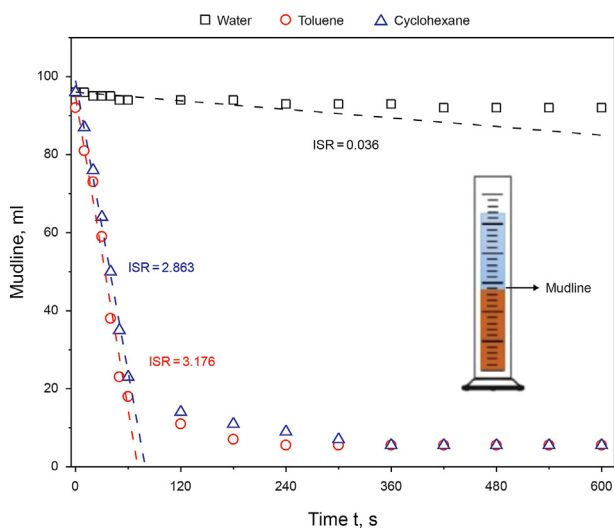


Fig. 4. Settling curves of prepared high molecular weight guar gum (HGG) in water (black squares, toluene (red circles) and cyclohexane (blue triangles). Insert: schematic of mudline in sedimentation tests in a graduated cylinder.

### 3.4. The effect of solvent mixtures on the size of water droplets and HGG aggregates

The impact of solvent effect (i.e., aromaticity of solvent) on the size of aggregates for both water droplets and HGG is further investigated by FBRM. The kinetic of aggregates formation (e.g., mean size value of water droplets and HGG aggregates in different solvents as functions of water and HGG dosages and time, respectively) is shown in Fig. 5a and b. As shown in Fig. 5a, the mean size of water droplets in all the solvents follows a similar trend, where a high-water dosage yields a large mean size of water droplets, especially in the dosage of 0.5–1.5 vol%. On the other hand, unlike the settling rate, the aromaticity of solvent does have effect on the size of water droplets, where a higher aromaticity of solvent yields smaller size of water droplets at the same water dosage. Interestingly, when HGG was added in the solvents, the trend on the mean size of HGG particles is more complicated as shown in Fig. 5b. The size of HGG particles in all the solvents are more or less same at HGG dosages over 0.75 vol% suggesting the high dosage has little effect on the mean size of HGG particles. Those HGG particles are likely dispersed well, and no homo-aggregation is formed in the solvents under 1100 rpm mixing. On the other hand, the mean size of HGG particles is largest in 3:2 T/Ch followed by 2:3 T/Ch, toluene and cyclohexane indicating the response of HGG particles in solvent may be governed by different mechanisms to water droplets.

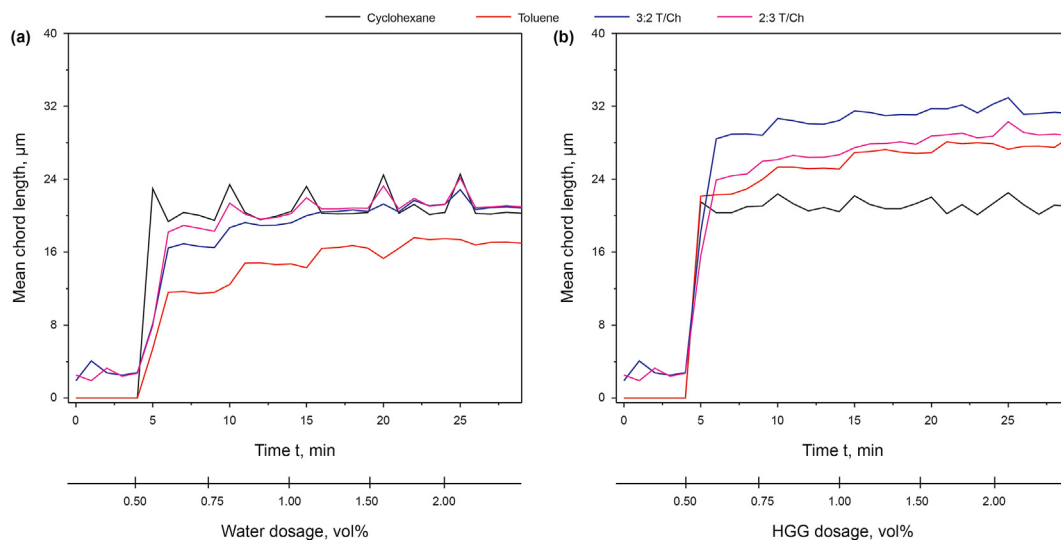


Fig. 5. Effect of solvent and solvent mixture on aggregate formation varying the amount of a) DI water and b) prepared HGG dosages.

Nevertheless, large HGG particles observed in mixing solvent (i.e., 3:2 T/Ch) is possibly a benefit to accelerate the settling of fine solids in bitumen and is discussed in the settling experiment next.

Table 1 shows the mean chord length and total No Weight counts of DI water droplets and HGG aggregates formed when 0.75 vol% of each additive is added to solvents. The total counts for HGG particles in all measured solvents are more or less same, though the mean size of HGG particles is dependent of solvent type. Unlike the HGG particles, the total counts of water droplets in solvents shows a correlation to the solvent type and emulsion stability, where the highest total counts are observed in toluene (stable emulsion) and lowest in cyclohexane consistent (unstable emulsion) as discussed previously in 3.1.

### 3.5. Solvent mixture effect on aggregate size in bituminous slurry

The kinetics of aggregates formation of water and HGG in solvent-diluted bitumen slurries (i.e., bitumen with 0.66 wt% fine solids in toluene, cyclohexane or solvent mixtures) were studied. A 0.75 vol% of DI water or HGG was chosen to be added in the following experiments, as it is the lowest dosage to give reasonable size for both HGG and water droplets in solvents. To analyze aggregate formation after stirring and during settling, two measurements are taken: one measurement is done immediately after the stirring speed is reduced and the second measurement is taken at 5 min after the first measurement. As expected, total counts of aggregates reduced notably in both DI water and HGG in all measured solvents (Figs. 6 and 7), and an estimated decrease of 51% and 69% in cyclohexane and toluene, respectively, is observed in

Table 1

Mean Chord lengths and Total counts of DI water droplets and HGG aggregates when 0.75 vol% of each additive is added to toluene, cyclohexane and solvent mixtures, without bitumen.

Solvent	Mean chord length, $\mu\text{m}$		Total counts (No Weight)	
	DI water	HGG	DI water	HGG
Toluene	12.45	25.32	159	97
Cyclohexane	21.81	22.38	94	98
3:2 T/Ch	18.70	30.66	120	93
2:3 T/Ch	21.36	26.16	113	96

comparison with 1100 rpm mixing (data from Fig. 3 and Table S1). In addition, Tables 2 and 3 provide the total counts (No Weight) in three distinct regions of 1–10, 11–20 and 21–60  $\mu\text{m}$ .

Fig. 6a shows the size distribution of aggregates right after reducing the stirring speed from 1100 rpm to 20 rpm. Significant counts can be found between the 11–60  $\mu\text{m}$  ranges, in pure cyclohexane, having comparable counts in both the 11–20 and 21–60  $\mu\text{m}$  ranges. The pure toluene system shows high aggregate counts in the smaller chord length range, especially in the 1–10  $\mu\text{m}$  size range. In mixed solvent systems, a higher content of toluene results in the defined peak in the smaller chord lengths (~5–12  $\mu\text{m}$ ), although the sum of the aggregates in the other range (21–60  $\mu\text{m}$ ) can be considered significant. When the content of cyclohexane surpasses toluene (2:3 T/Ch), significant counts can be found between 1 and 20  $\mu\text{m}$ , but this system had a considerably higher number of aggregates in the larger size range (21–60  $\mu\text{m}$ ) than toluene and 3:2 T/Ch. Although a significant amount of aggregates below 20  $\mu\text{m}$  was observed in both T/Ch solvents, the result of 3:2 T/Ch approximately resembles that of toluene, while that of 2:3 T/Ch resembles that of cyclohexane. Despite the considerable decrease in the amount of aggregates, cyclohexane containing systems appear to have, on average, slightly higher counts of aggregates.

After 5 min of settling, significant reduction of counts is found in all solvent systems as shown in Fig. 6b and Table 2. However, results in solvent mixtures show fewer counts of aggregates in a broader range of sizes (>10  $\mu\text{m}$ ), compared to the results for pure solvent systems. The majority of the aggregates in the cyclohexane system are in the 11–20  $\mu\text{m}$  range, although a comparable number of aggregates can be found in the upper limit of the lower range (1–10  $\mu\text{m}$ ). Most aggregates in toluene continue to be present between 1 and 10  $\mu\text{m}$  in addition to having significantly smaller counts of aggregates up to 60  $\mu\text{m}$ .

The previously described procedure is repeated with 0.75 vol% of diluted HGG, and the results are shown in Fig. 7 and Table 3, respectively. Overall, significant counts were found in the small size range. Fig. 7a shows that aggregates in pure toluene have higher counts in a narrow range of chord lengths (3–20  $\mu\text{m}$ ) that is in contrary to aggregates in pure cyclohexane with a wide range of sizes (8–35  $\mu\text{m}$ ) and lower counts. This is the main difference from water aided aggregates. In mixed solvent systems, random peaks above 50  $\mu\text{m}$  can be found. In the 3:2 T/Ch system, an array of chord lengths varying from 5 to 90  $\mu\text{m}$  is observed, yet, significant counts

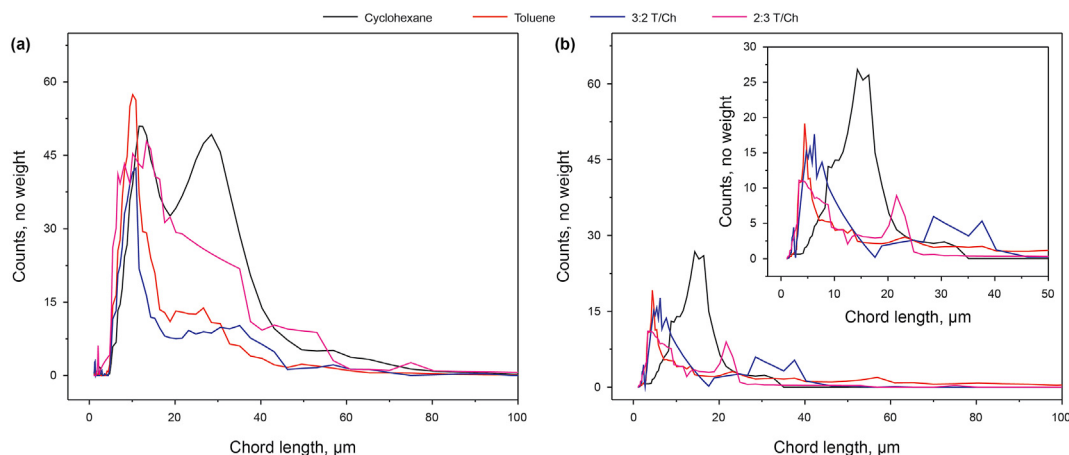


**Fig. 6.** FBRM results of the effect of solvent and solvent mixture on aggregate formation with 0.75 vol% of DI water immediately after stirring, a) before settling and b) after 5 min of settling. Insert: close-up look at Fig. 6b.

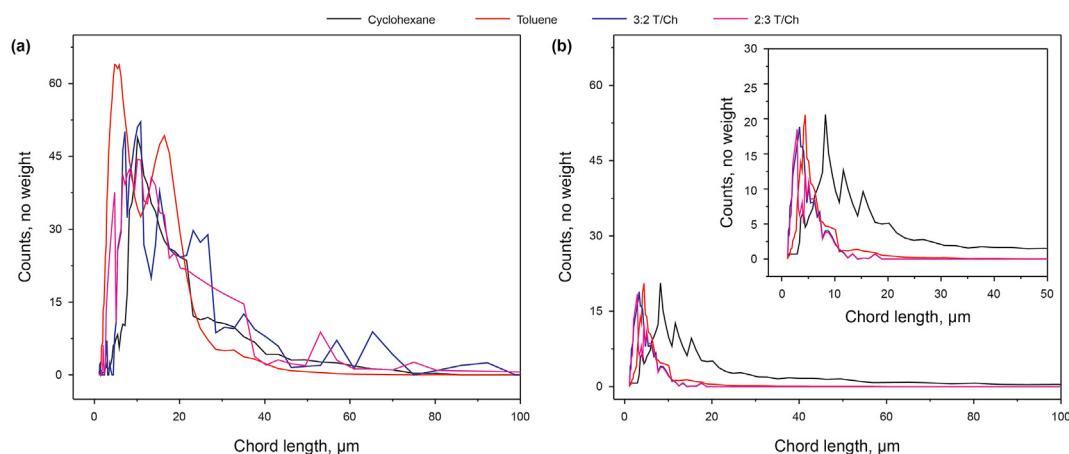


**Fig. 7.** FBRM results: effects of solvent on aggregate formation with addition of 0.75 vol% HGG, a) before settling and b) after 5 min of settling. Insert: close-up look at Fig. 7b.

**Table 2**

Total counts of aggregates after introducing 0.75 vol% of DI water when stirring speed is reduced to promote settling and after 5 min of settling in toluene, cyclohexane and solvent mixtures.

Total Counts (No Weight)								
Solvent	Before Settling				5 min after settling			
	Chord length, μm			Total	Chord length, μm			Total
	1–10	11–20	21–60		1–10	11–20	21–60	
Toluene	350	248	107	705	11	60	78	249
Cyclohexane	200	420	409	1029	92	180	19	291
3:2 T/Ch	272	156	102	530	178	27	29	234
2:3 T/Ch	250	235	163	648	191	35	22	248

from this system are found principally from 5 to 27 μm. In 2:3 T/Ch, a standalone peak in ~5 μm followed by a count-decreasing peak ranging between 8 and 36 μm are identified, however, significant counts are also observed in ~53 μm.

Once again counts in all systems have decreased considerably after 5 min of settling. Comparing Figs. 6b and 7b, HGG accelerates the settling because of high molecular weight inherit to HGG (Jayawardena et al., 2015), hence lower counts are observed in all systems with a more uniform size distribution. The pure cyclohexane system has larger aggregates (5–21 μm), similar to the case when water was used as a process aid. The number of aggregates in

pure toluene are comparable with the ones found in pure cyclohexane, although the chord length (3–9 μm) is much smaller. In mixed solvent systems, both showed slightly fewer counts than pure solvent system, with a uniform average chord length (2–8 μm).

The size and quantity of fine solids and aggregates can be seen in Fig. 8, where microscopic images of the supernatant when HGG is used, immediately after lowering stirring speed and 5 min afterwards. Fig. 8a–d shows the fine solids in the supernatant taken immediately after the stirring rate was reduced to 20 rpm, while Fig. 8e–h represents the images of the supernatant taken after

**Table 3**

Total counts of aggregates after introducing 0.75 vol% of HGG when stirring speed is reduced to promote settling and after 5 min of settling in toluene, cyclohexane and solvent mixtures.

Total Counts (No Weight)								
Solvent	Before Settling				5 min after settling			
	Chord length, $\mu\text{m}$			Total	Chord length, $\mu\text{m}$			Total
	1–10	11–20	21–60		1–10	11–20	21–60	
Toluene	244	310	122	676	160	8	1	169
Cyclohexane	674	243	49	966	159	75	39	273
3:2 T/Ch	265	142	77	484	146	2	0	148
2:3 T/Ch	239	160	113	512	142	3	0	155

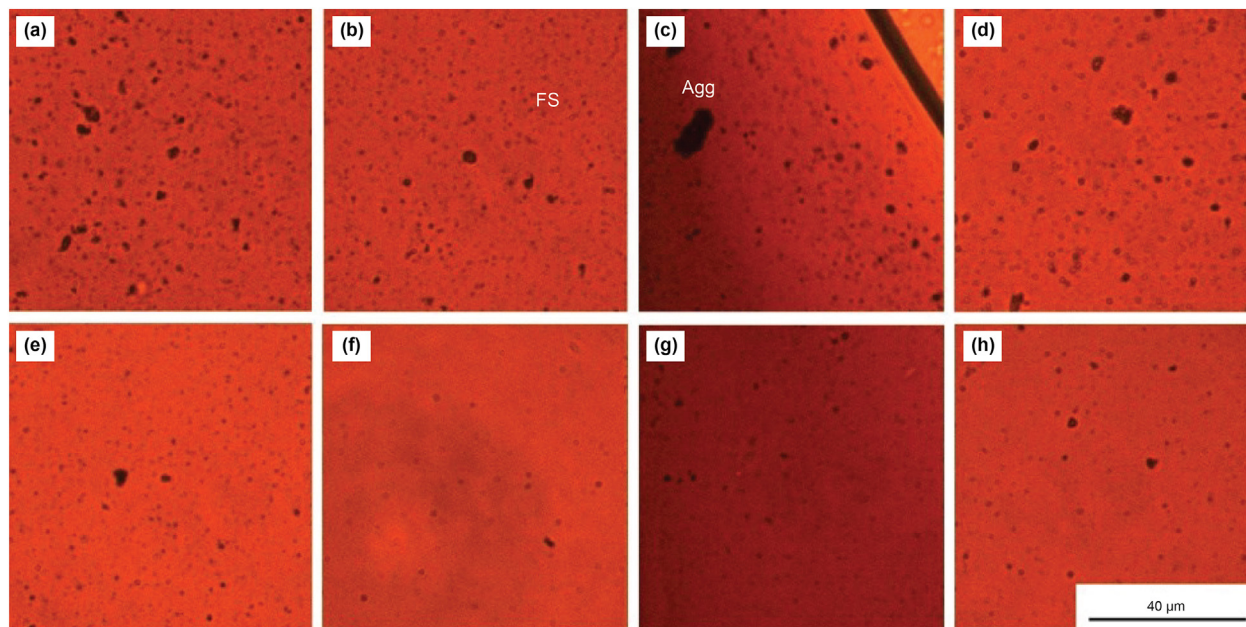


**Fig. 8.** Micrographs of supernatant after treating the slurry with 0.75 vol% of HGG, (a–d) immediately after stopping stirring and (e–h) after 5 min of settling, (from left to right) in cyclohexane, toluene, 3:2 T/Ch and 2:3 T/Ch, respectively. FS: fine sol.

5 min of settling. Overall, Fig. 8 validates the results found in the FBRM tests for HGG-treated solvent-diluted bitumen. The low content of HGG due to the initial dilution (200 ppm) cannot be appreciated. The presence of large aggregates ( $>30 \mu\text{m}$ ) when solvent mixtures are used after the stirring speed is slowed down is observed in Fig. 8c and d. This confirms the peaks found between the 30–40  $\mu\text{m}$  chord lengths shown in Fig. 7a. After 5 min of settling, the supernatants contain less aggregates as shown in the microscopic images, which is consistent with the low counts measured in the FBRM tests. In addition, the supernatant with higher number of solids appears to be cyclohexane that is consistent with FBRM results.

### 3.6. Final solid content in supernatant

A design scenario of a potential NAE process is that the NAE bitumen would have a residence time of 30 min in a settling tank. Therefore, supernatant samples are taken after 30 min of settling. Ashing and hot filtration are performed to obtain the final solid content in the supernatant. As shown in Fig. 9, in the control experiment without additives, the solid content in bitumen remains constant independent of the solvents tested. When water or HGG was added, the solids content in bitumen decreased. The addition of water has shown the benefit on the reduction of solid

contents in bitumen, while a slightly better performance was observed in mixed solvents than single solvent cases. Meanwhile, the addition of HGG has shown a remarkable reduction in solid content in all solvents, particularly in mixed solvents, which was verified by both ashing and hot filtration methods. Among the solvents, 3:2 T/Ch was identified as the most effective solvent to reduce solid content from 0.66 wt% to 0.49 wt% for DI water and to 0.10 wt% for HGG at 0.75 vol%, respectively.

Because of the promising results from HGG, the effect of HGG concentration on the solids content in bitumen was further investigated with the same settling procedures and the results are shown in Fig. 10. The pure cyclohexane system shows that increasing the concentration of HGG to 1 vol% can decrease the solid content to some extent, however, a further increase of concentration of the HGG could not benefit the decrease of solids content. This phenomenon was observed in all solvents likely due to the thickening properties of HGG, which, in high quantities, might counteract its ability to form aggregates and further settle. In toluene, a 0.75 vol% HGG resulted in the lowest solids content of about 0.3 wt%.

In mixed solvent systems, the results are overall better than pure solvents. In 2:3 T/Ch system, a significant improvement was observed with a HGG content of 0.75 vol%. Meanwhile, the best performance was obtained in 3:2 T/Ch system at all measured HGG

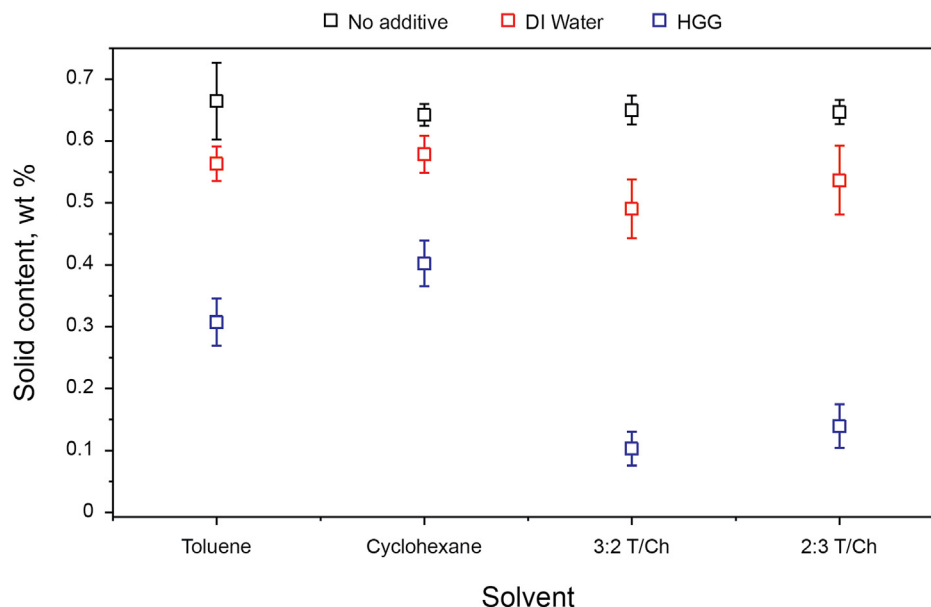


Fig. 9. Solid content in dry bitumen from supernatant without additive and after treating with DI water (0.75 vol%) and HGG (0.75 vol%) in cyclohexane, toluene and their mixtures.

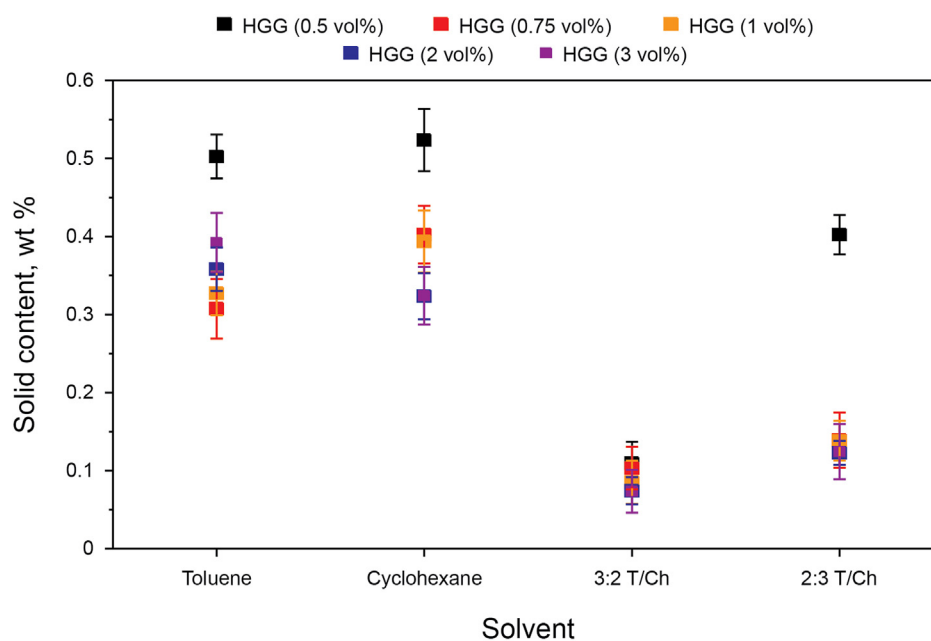


Fig. 10. Solid content in the supernatant after treatment with different dosages of HGG in toluene, cyclohexane and their mixtures.

concentrations, where a solid content in bitumen (<0.1 wt%) was achieved. Coincidentally, the size of HGG aggregates in pure 3:2 T/Ch solvent (without bitumen/solids) is largest among the tested solvents as discussed previously indicating that an optimized size of HGG aggregates may be required for best treatment performance. A further investigation on the effect of size of HGG aggregates would be an interesting direction to pursue in the future work. In addition, a general consensus in bitumen product cleaning is to find an efficient additive or chemical aid to aggregate the fine solids for easy removal, however, the results from our studies demonstrated that the composition of solvent medium plays an equally important role in fine solids removal in bitumen product cleaning in addition to the use of proper process aids. It opens new strategies

to deal with the challenge of removing fine solids from bitumen product.

#### 4. Conclusions

Hydrophilic settling aids in organic media have shown promising results towards the settling of fine solids in the bitumen extracted from oil sands using non-aqueous solvents. This work aims to provide a feasible way to improve fine solids settling for further removal by tuning the aromatic content of the solvent when DI water and guar gum are used to promote fine solids settling. Toluene, cyclohexane and their mixtures in 3:2 and 2:3 (v/v) toluene/cyclohexane are used to study the aromaticity effect in the



settling of fine solids in diluted bitumen. The results from focused beam reflectance measurements show that the aromaticity of solvent does affect the size of water droplets, where a higher aromaticity of solvent yields smaller size of water droplets at the same water dosage. The size of HGG aggregates is largest in 3:2 T/Ch followed by 2:3 T/Ch, toluene and cyclohexane, indicating that the response of HGG particles in solvent may be governed by different mechanisms to water droplets. In bitumen-diluted systems, significant reductions of total counts were observed from both FBRM and microscope results, after settling aid treatment. This was further confirmed with by the results of supernatant solid content in supernatants determination, in which HGG showed a better performance than water in all tested solvents. A fine solid content reduction of ~80% at 3:2 T/Ch was observed. The results provide useful insights into the development of effective methods to remove the fine solids from bitumen produced from the NAE process.

## Acknowledgements

The authors acknowledge the financial support from Institute for Oil Sands Innovation (IOSI), Imperial Oil, the Natural Sciences and Engineering Research Council of Canada (NSERC), the Canada Foundation for Innovation (CFI), the Future Energy Systems under the Canada First Research Excellence Fund and the Canada Research Chairs Program to the research work. The authors are also grateful for the technical support from IOSI lab, particularly from Lisa Brandt and Brittany MacKinnon.

## Appendix A. Supplementary data

Supplementary data to this article can be found online at <https://doi.org/10.1016/j.petsci.2021.09.013>.

## References

- American Petroleum institute, 2015. Standard Test Method for Sediment in Crude Oil by Membrane Filtration Astm, pp. 8–11. <https://doi.org/10.1067/mem.2001.117272>.
- Anderson, W.G., 1985. Wettability Literature Survey - Part 1: rock-Oil-Brine interactions and the effects of core handling on wettability. Soc. Pet. Eng. AIME. SPE. (October), 1125–1144. <https://doi.org/10.2118/13932-PA>.
- Autochem, M., 2006. Particle Characterization Track Particles in Real Time Optimize and Monitor Processes. Mettler-Toledo AutoChem, Inc.
- Chakraborti, R.K., Gardner, K.H., Atkinson, J.F., Van Benschoten, J.E., 2003. Changes in fractal dimension during aggregation. Water Res. 37, 873–883. [https://doi.org/10.1016/S0043-1354\(02\)00379-2](https://doi.org/10.1016/S0043-1354(02)00379-2).
- Geramian, M., Osacky, M., Ivey, D.G., Liu, Q., Etsell, T.H., 2016. Effect of swelling clay minerals (montmorillonite and illite-Smectite) on nonaqueous bitumen extraction from Alberta oil sands. Energy & Fuels 30, 8083–8090. <https://doi.org/10.1021/acs.energyfuels.6b01026>.
- Gupta, B Sen, Ako, J.E., 2005. Application of guar gum as a flocculant aid in food processing and potable water treatment. Eur. Food Res. Technol. 221, 746–751. <https://doi.org/10.1007/s00217-005-0056-4>.
- Hall, A.C., Collins, S.H., Melrose, J.C., 1983. Stability of aqueous wetting films in Athabasca tar sands. Soc. Petrol. Eng. J. 23, 249–258. <https://doi.org/10.2118/10626-PA>.
- Hasan, A.M.A., Abdel-Raouf, M.E., 2018. Applications of guar gum and its derivatives in petroleum industry: a review. Egypt. J. Pet. Egyptian Petroleum Research Institute 27, 1043–1050. <https://doi.org/10.1016/j.ejpe.2018.03.005>.
- Hogshead, C.G., Manias, E., Williams, P., Lupinsky, A., Painter, P., 2011. Studies of bitumen-silica and oil-silica interactions in ionic liquids. Energy & Fuels 25, 293–299. <https://doi.org/10.1021/ef101404k>.
- Hooshari, A., Uhlik, P., Ivey, D.G., Liu, Q., Etsell, T.H., 2012a. Clay minerals in nonaqueous extraction of bitumen from Alberta oil sands: Part 1. Nonaqueous extraction procedure. Fuel Process. Technol. 94, 80–85. <https://doi.org/10.1016/j.fuproc.2011.10.008>.
- Hooshari, A., Uhlik, P., Liu, Q., Etsell, T.H., Ivey, D.G., 2012b. Clay minerals in nonaqueous extraction of bitumen from Alberta oil sands: Part 2. Characterization of clay minerals. Fuel Process. Technol. 96, 183–194. <https://doi.org/10.1016/j.fuproc.2011.10.010>.
- International Petroleum Test methods, 2008. Standard test method for ash from petroleum products. Manual on Hydrocarbon Analysis. <https://doi.org/10.1520/MNL10845M>, 141-141–3, sixth ed.
- Jayawardena, B., Pantithavidana, D., Sameera, W., 2015. Polysaccharides in solution: experimental and computational studies. Intech open 2, 64. <https://doi.org/10.5772/intechopen.69863>.
- Li, Z., Lu, P., Zhang, D., Chen, G., Zeng, S., He, Q., 2016. Population balance modeling of activated sludge flocculation: investigating the influence of extracellular polymeric substances (EPS) content and zeta potential on flocculation dynamics. Separ. Purif. Technol. 162, 91–100. <https://doi.org/10.1016/j.seppur.2016.02.011>.
- Liu, J., Cui, X., Huang, J., Xie, L., Tan, X., Liu, Q., et al., 2019a. Understanding the stabilization mechanism of bitumen-coated fine solids in organic media from non-aqueous extraction of oil sands. Fuel 242, 255–264. <https://doi.org/10.1016/j.fuel.2019.01.029>.
- Liu, J., Cui, X., Santander, C., Tan, X., Liu, Q., Zeng, H., 2019b. Destabilization of fine solids suspended in oil media through wettability modification and water-assisted agglomeration. Fuel 254, 115623. <https://doi.org/10.1016/j.fuel.2019.115623>.
- Liu, J., Wang, J., Huang, J., Cui, X., Tan, X., Liu, Q., et al., 2017. Heterogeneous distribution of adsorbed bitumen on fine solids from solvent-based extraction of oil sands probed by AFM. Energy & Fuels 31, 8833–8842. <https://doi.org/10.1021/acs.energyfuels.7b00396>.
- Liu, J., Xu, Z., Masliyah, J., 2003. Studies on bitumen-silica interaction in aqueous solutions by atomic force microscopy. Langmuir 19, 3911–3920. <https://doi.org/10.1021/la0268092>.
- Liu, J., Xu, Z., Masliyah, J., 2008. Interaction between bitumen and fines in oil sands extraction system: implication to bitumen recovery. Can. J. Chem. Eng. 82, 655–666. <https://doi.org/10.1002/cjce.5450820404>.
- Lu, Q., Huang, J., Liu, Y., Zeng, H., Yan, B., Xie, L., 2016. A two-step flocculation process on oil sands tailings treatment using oppositely charged polymer flocculants. Sci. Total Environ. 565, 369–375. <https://doi.org/10.1016/j.scitotenv.2016.04.192>.
- Ma, X., Pawlik, M., 2007. Role of background ions in guar gum adsorption on oxide minerals and kaolinite. J. Colloid Interface Sci. 313, 440–448. <https://doi.org/10.1016/j.jcis.2007.04.075>.
- Mahmoud, N.M., 2000. Physico-chemical Study on Guar Gum [MSc Thesis]. Department of Chemistry, University of Khartoum.
- Narchi, I., Vial, C., Djelveh, G., 2009. Effect of protein-polysaccharide mixtures on the continuous manufacturing of foamed food products. Food Hydrocolloids 23, 188–201. <https://doi.org/10.1016/j.foodhyd.2007.12.010>.
- Natarajan, A., Xie, J., Wang, S., Liu, Q., Masliyah, J., Zeng, H., et al., 2011. Understanding molecular interactions of asphaltene in organic solvents using a surface force apparatus. J. Phys. Chem. 115, 16043–16051. <https://doi.org/10.1021/jp2039674>.
- Nikakhtari, H., Vagi, L., Choi, P., Liu, Q., Gray, M.R., 2013. Solvent screening for non-aqueous extraction of Alberta oil sands. Can. J. Chem. Eng. 91, 1153–1160. <https://doi.org/10.1002/cjce.21751>.
- Nikakhtari, H., Wolf, S., Choi, P., Liu, Q., Gray, M.R., 2014. Migration of fine solids into product bitumen from solvent extraction of Alberta oil sands. Energy & Fuels 28, 2925–2932. <https://doi.org/10.1021/ef500021y>.
- Painter, P., Williams, P., Mannebach, E., 2010. Recovery of bitumen from oil or tar sands using ionic liquids. Energy & Fuels 24, 1094–1098. <https://doi.org/10.1021/ef9009586>.
- Pal, K., Nogueira Branco, L.D.P., Heintz, A., Choi, P., Liu, Q., Seidl, P.R., et al., 2015. Performance of solvent mixtures for non-aqueous extraction of Alberta oil sands. Energy & Fuels 29, 2261–2267. <https://doi.org/10.1021/ef502882c>.
- Pal, S., Mal, D., Singh, R.P., 2007. Synthesis and characterization of cationic guar gum: a high performance flocculating agent. J. Appl. Polym. Sci. 105, 3240–3245. <https://doi.org/10.1002/app.26440>.
- Park, J.M., Kwon, D.J., Wang, Z.J., Byun, J.H., Lee, H.I., Park, J.K., et al., 2014. Novel method of electrical resistance measurement in structural composite materials for interfacial and dispersion evaluation with nano- and hetero-structures. Mater. Res. Soc. Symp. Proc. 1700, 37–46. <https://doi.org/10.1557/opl.2014.537>.
- Schäfer, M., Polke, R., Rädle, M., Sachweh, B., Scholz, N., Heffels, C., 2002. Control of particulate processes by optical measurement techniques. Part. Part. Syst. Char. 15, 211–218. [https://doi.org/10.1002/\(SICI\)1521-4117\(199810\)15:5%3C211::AID-PPSC211%3E3.0.CO;2-H](https://doi.org/10.1002/(SICI)1521-4117(199810)15:5%3C211::AID-PPSC211%3E3.0.CO;2-H).
- Sharma, G., Sharma, S., Kumar, A., Al-muhtaseb, A.H., Naushad, M., Ghfar, A.A., et al., 2018. Guar gum and its composites as potential materials for diverse applications: a review. Carbohydr. Polym. 199, 534–545. <https://doi.org/10.1016/j.carbpol.2018.07.053>.
- Smith, D.E., Wang, Y., Chaturvedi, A., Whitley, H.D., Zhuang, Y., Liu, X., et al., 2011. Molecular simulations of the pressure, temperature, and chemical potential dependencies of clay swelling. Energy & Fuels. American Chemical Society 110, 3125–3134. <https://doi.org/10.1021/acs.energyfuels.7b03686>.
- Sparks, B.D., Meadus, F.W., 1981. A study of some factors affecting solvent losses in the solvent extraction-spherical agglomeration of oil sands. Fuel Process. Technol. 4, 251–264. [https://doi.org/10.1016/0378-3820\(81\)90002-3](https://doi.org/10.1016/0378-3820(81)90002-3).
- Sparks, B.D., Meadus, F.W., Hoefele, E.O., 1988. Solvent extraction spherical agglomeration of oil sands. United States Patent 1–23. [https://doi.org/10.1016/0160-4120\(88\)90049-9](https://doi.org/10.1016/0160-4120(88)90049-9).
- Tadayyon, A., Rohani, S., 1998. Determination of particle size distribution by Par-Tec® 100: modeling and experimental results. Part. Part. Syst. Char. 15, 127–135. [https://doi.org/10.1002/\(SICI\)1521-4117\(199817\)15:3%3C127::AID-PPSC127%3E3.0.CO;2-B](https://doi.org/10.1002/(SICI)1521-4117(199817)15:3%3C127::AID-PPSC127%3E3.0.CO;2-B).
- Tan, X., Fenniri, H., Gray, M.R., 2009. Water enhances the aggregation of model asphaltene in solution via hydrogen bonding. Energy & Fuels 23, 9080–9086.

- <https://doi.org/10.1021/ef900228s>.
- Tan, X., Reed, A.H., Hu, L., Zhang, G., Furukawa, Y., 2013. Flocculation and particle size analysis of expansive clay sediments affected by biological, chemical, and hydrodynamic factors. *Ocean Dynam.* 64, 143–157. <https://doi.org/10.1007/s10236-013-0664-7>.
- Thombare, N., Jha, U., Mishra, S., Siddiqui, M.Z., 2016. Guar gum as a promising starting material for diverse applications: a review. *Int. J. Biol. Macromol.* 88, 361–372. <https://doi.org/10.1016/j.ijbiomac.2016.04.001>.
- Tian, Y., McGill, W.B., Whitcombe, T.W., Li, J., 2019. Ionic liquid-enhanced solvent extraction for oil recovery from oily sludge. *Energy & Fuels* 33, 3429–3438. <https://doi.org/10.1021/acs.energyfuels.9b00224>.
- Towle, G.A., Whistler, R.L., 2012. Chemical Modification of Gums. *Industrial Gums: Polysaccharides and Their Derivatives*, third ed. <https://doi.org/10.1016/B978-0-08-092654-4.50007-3>
- Vajihinejad, V., Soares, J.B.P., 2018. Monitoring polymer flocculation in oil sands tailings: a population balance model approach. *Chem. Eng. J.* 346, 447–457. <https://doi.org/10.1016/j.cej.2018.04.039>.
- Yan, N., Gray, M.R., Masliyah, J.H., 2001. On water-in-oil emulsions stabilized by fine solids. *Colloids Surf., A* 193, 97–107. [https://doi.org/10.1016/S0927-7757\(01\)00748-8](https://doi.org/10.1016/S0927-7757(01)00748-8).
- Zahabi, A., Gray, M.R., Dabros, T., 2012. Kinetics and properties of asphaltene adsorption on surfaces. *Energy & Fuels* 26, 1009–1018. <https://doi.org/10.1021/ef2014698>.